Kinetics and Mechanism of the Formation and Acid Dissociation of Cobalt(II), Nickel(II), and Copper(II) Complexes with the Highly Enolized β-Diketone 3-(*N*-Acetylamido)pentane-2,4-dione (=Hamac) in Aqueous Solution†

Jürgen Hirsch,‡ Helmut Paulus,§ and Horst Elias*,‡

Institut für Anorganische Chemie and Fachbereich Materialwissenschaft, Technische Hochschule Darmstadt, Petersenstrasse 18, D-64289 Darmstadt, Federal Republic of Germany

Received March 8, 1995⊗

The β-diketone Hamac = 3-(*N*-acetylamido)pentane-2,4-dione was characterized by potentiometric, spectrophotometric, and kinetic methods. In water, Hamac is very soluble (2.45 M) and strongly enolized, with [enol]/[ketone] = 2.4 ± 0.1. The pK_a of Hamac is 7.01 ± 0.07, and the rate constants for enolization, k_e, and ketonization, k_k, at 298 K are 0.0172 ± 0.0004 s^{-1} and 0.0074 ± 0.0015 s^{-1}, respectively. An X-ray structure analysis of the copper(II) complex $Cu(amac)_2$·toluene (=$C_{21}H_{28}CuN_2O_6$; monoclinic, *C*2/*c*; *a* = 20.434(6), *b* = 11.674(4), *c* = 19.278(6) Å; β = 100.75(1)°; *Z* = 8; R_w = 0.0596) was carried out. The bidentate anions $amac^-$ coordinate the copper via the two diketo oxygen atoms to form a slightly distorted planar CuO_4 coordination core. Rapid-scan stopped-flow spectrophotometry was used to study the kinetics of the reaction of divalent metal ions M^{2+} (M = Ni,Co,Cu) with Hamac in buffered aqueous solution at variable pH and *I* = 0.5 M ($NaClO_4$) under pseudo-first-order conditions ($[M^{2+}]_0 \gg [Hamac]_0$) to form the mono complex $M(amac)^+$. For all three metals the reaction is biphasic. The absorbance/time data can be fitted to the sum of two exponentials, which leads to first-order rate constants k_f (fast initial step) and k_s (slower second step). The temperature dependence of k_f and k_s was measured. It follows from the kinetic data that (i) the keto tautomer of Hamac, HK, does not react with the metal ions M^{2+}, (ii) the rate constant k_f increases linearly with $[M^{2+}]_0$ according to $k_f = k_0 + k_2[M^{2+}]_0$, and (iii) the rate constant k_s does not depend on $[M^{2+}]_0$ and describes the enolization of the unreactive keto tautomer HK. The pH dependence of the second-order rate constant k_2 reveals that both the enol tautomer of Hamac, HE, and the enolate, E^-, react with M^{2+} in a second-order reaction to form the species $M(amac)^+$. At 298 K rate constants k_{HE} are 18 ± 6 (Ni), 180 ± 350 (Co), and (9 ± 5) × 10^4 (Cu) M^{-1} s^{-1} and rate constants k_E are 924 ± 6 (Ni), (7.4 ± 0.6) × 10^4 (Co), and (8.4 ± 0.2) × 10^8 (Cu) M^{-1} s^{-1}. The acid dissociation of the species $M(amac)^+$ is triphasic. Very rapid protonation (first step) leads to $M(Hamac)^{2+}$, which is followed by dissociation of $M(Hamac)^{2+}$ and $M(amac)^+$, respectively (second step). The liberated enol Hamac ketonizes (third step). The mechanistic implications of the metal dependence of rate constants k_{HE}, k_E, k_{-HE}, and k_{-E} are discussed.

Introduction

The reaction of metal ions with β-diketones are more complicated than many other complex formation reactions in which the rate of complexation is controlled by the rate of solvent exchange. The complications arise from the fact that β-diketones HL are subject to a keto/enol tautomerism according to (1). The keto tautomer HK is in equilibrium with the enol

$$HK \underset{k_k}{\overset{k_e}{\rightleftharpoons}} HE \tag{1a}$$

$$HK \rightleftharpoons H^+ + E^- \rightleftharpoons HE \tag{1b}$$

HE, and both tautomers can dissociate to form the enolate E^-, so that a given metal ion can react with either HK, HE, or E^-.

The kinetics and mechanisms of complex formation with β-diketones have been thoroughly discussed by Hynes in a recent review.[1] In particular, the work carried out by Pearson and Anderson,[2] Sutin et al.,[3,4] and Hynes et al.[5−18] provides a lot of mechanistic information concerning reactions 2a−c. It is

$$M^{q+} + HK \rightarrow ME^{(q-1)+} + H^+ \tag{2a}$$

$$M^{q+} + HE \rightarrow ME^{(q-1)+} + H^+ \tag{2b}$$

$$M^{q+} + E^- \rightarrow ME^{(q-1)} \tag{2c}$$

nevertheless still a matter of dispute[1] as to which ligand-based and/or metal-based factors control the intimate mechanism of these reactions.

† Dedicated to Prof. Dr. K.-H. Lieser on the occasion of his 75th birthday.
‡ Institut für Anorganische Chemie.
§ Fachbereich Materialwissenschaft.
⊗ Abstract published in *Advance ACS Abstracts,* March 1, 1996.

(1) Hynes, M. J. *Rev. Inorg. Chem.* **1990**, *11*, 21.
(2) Pearson, R. G.; Anderson, O. P. *Inorg. Chem.* **1970**, *9*, 39.
(3) Jaffe, M. R.; Fay, D. P.; Cefola, M.; Sutin, N. *J. Am. Chem. Soc.* **1971**, *93*, 2878.
(4) Fay, D. P.; Nichols, A. R., Jr.; Sutin, N. *Inorg. Chem.* **1971**, *10*, 2096.
(5) Hynes, M. J.; O'Regan, B. D. *J. Chem. Soc., Dalton Trans.* **1976**, 1200.
(6) Hynes, M. J.; O'Regan, B. D. *Proc. R. Irish Acad.* **1977**, *77B*, 285.
(7) Hynes, M. J.; O'Regan, B. D. *J. Chem. Soc., Dalton Trans.* **1979**, 162.
(8) Hynes, M. J.; O'Regan, B. D. *J. Chem. Soc., Dalton Trans.* **1980**, 7.
(9) Hynes, M. J.; O'Regan, B. D. *J. Chem. Soc., Dalton Trans.* **1980**, 1502.
(10) Hynes, M. J.; O'Shea, M. T. *J. Chem. Soc., Dalton Trans.* **1983**, 331.
(11) Hynes, M. J.; O'Shea, M. T. *Inorg. Chim. Acta* **1983**, *73*, 201.
(12) Ando, I.; Yoshizumi, K.; Kazuhisa, I.; Ujimoto, K.; Kurihara, H. *Bull. Chem. Soc. Jpn.* **1983**, *56*, 1368.
(13) Hynes, M. J.; O'Mara, C.; Kelly, D. F. *Inorg. Chim. Acta* **1986**, *120*, 131.
(14) Hernando, J. M.; Blanco, C.; Prieto, T. *Bull. Soc. Chim. Fr.* **1987**, 775.
(15) Hynes, M. J.; Kelly, D. F. *J. Chem. Soc., Dalton Trans.* **1988**, 905.
(16) Hynes, M. J.; Mooney, M. T. *Proc. R. Irish Acad.* **1989**, *89 B*, 441.
(17) Blanco, C.; Hynes, M. J. *Bull. Soc. Chim. Fr.* **1989**, 611.
(18) Blanco, C.; Hynes, M. J. *J. Chim. Phys.* **1989**, *86*, 1989.

0020-1669/96/1335-2343$12.00/0

Our work[19] on the coordination chemistry of "isonitrosoacetylacetone" (=3-(hydroxyimino)pentane-2,4-dione) led us to the substituted β-diketone 3-(*N*-acetylamido)pentane-2,4-dione = Hamac,[20] the copper complex of which was prepared by

Hamac =

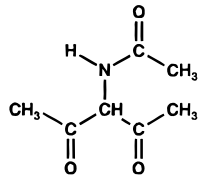

Fackler and Cotton.[21] This ligand is a remarkable β-diketone in that it is very soluble in water, much more strongly enolized than any of the β-diketones studied so far, and rather acidic. We decided to study the kinetics of mono complex formation according to (3) in aqueous solution for M = Co, Ni, and Cu

$$M^{2+} + \text{Hamac} \rightleftharpoons M(\text{amac})^{+} + H^{+} \qquad (3)$$

and thus contribute to the understanding of the mechanism of the enol-based and enolate-based reactions 2b and 2c.

Experimental Section

Chemicals. The various metal perchlorates and buffers (HMOPS,[20] HMES,[20] HLUS[20,22]) were reagent grade. The solvent water was purified by double distillation of deionized water in a quartz apparatus. The ligand Hamac (mp 99−100 °C) was prepared from Hacac[20] in a two-step procedure as described.[21,23]

Cu(amac)$_2$ and Cu(amac)$_2$·toluene. A solution of 0.65 g of Cu(AcO)$_2$·H$_2$O (3.25 mmol) in 25 mL of warm ethanol was slowly added to a solution of 1.02 g of Hamac (6.5 mmol) in 25 mL of warm ethanol. After 10 min of stirring at 60 °C, the hot green solution was filtered. Cooling of the filtrate led to a green precipitate, which was recrystallized from ethanol, washed with cyclohexane, and dried in vacuo over silica gel at 60 °C to yield crystalline Cu(amac)$_2$ (yield 40%; dec pt >150 °C). Cu(amac)$_2$·toluene was prepared analogously, with a 1:1 mixture of ethanol/toluene instead of ethanol serving as solvent. Cooling of the reaction mixture led to green needles of Cu(amac)$_2$·toluene (yield 40%; dec pt >180 °C).

The results of elemental analysis (C,H,N) of Hamac and the two copper complexes were in good agreement with calculated data. The magnetic moments of Cu(amac)$_2$ and Cu(amac)$_2$·toluene at 20 °C were found to be 1.91 and 1.93 μ_B, respectively. The solubility of Hamac (2.45 M) and Cu(amac)$_2$ (0.54 M) in water at 25 °C was determined spectrophotometrically.

Instrumentation. Magnetic susceptibility: magnetic susceptibility balance (Johnson-Matthey, type MSB-MKI). UV/vis spectra: diode array spectrophotometer (Hewlett-Packard, type 8451). pH: pH meter (Metrohm, type 654) in combination with a glass electrode (Ingold, type 405-88-S7), calibrated at I = 0.5 M ($NaClO_4$) to yield the relationship $-\log[H^+] = pH - 0.11$. Potentiometric titration: apparatus (Metrohm) consisting of potentiograph, automatic titrator, and Ag/AgCl reference glass electrode. Kinetic measurements: modified[24] stopped-flow spectrophotometer (Durrum, D 110) and rapid-scan stopped-flow spectrophotometer.[25]

pK_a of Hamac. The pK_a of the ligand in water (I = 0.5 M, $NaClO_4$) was determined by potentiometric and spectrophotometric titration with NaOH at 25 °C. The potentiometric method[26] led to pK_a = 7.08 and the spectrophotometric titration,[27] based on λ_{max}(Hamac) = 278 nm (ϵ = 6700 M^{-1} cm^{-1}) and λ_{max}(amac$^-$) = 296 nm (ϵ = 15 400 M^{-1} cm^{-1}), led to pK_a = 6.93. The mean of these two independent determinations is thus pK_a = 7.01 ± 0.07.

Stability Constants. Equilibrium constant K_1 for mono complex formation according to (3a) was determined by spectrophotometric

$$M^{2+} + \text{amac}^{-} \overset{K_1}{\rightleftharpoons} M(\text{amac})^{+} \qquad (3a)$$

titration of solutions of Hamac and the metal perchlorate (M = Co, Ni, Cu) and NaOH at I = 0.5 M ($NaClO_4$) and 298 K. Complex formation was monitored in the UV range as well as in the d−d range, as based on the following absorption data [λ_{max}, nm (ϵ_{max}, M^{-1} cm^{-1})]: Hamac, 278 (6700); amac$^-$, 296 (15 400); Co(amac)$^+$, 298 (9400) and 508 (14); Ni(amac)$^+$, 302 (12 350) and 648 (3.4); Cu(amac)$^+$, 302 (11 850) and 724 (32); Cu(amac)$_2$, 298 (22 600) and 648 (44). Computer fitting of the data[28] led to the following stability constants.

M	K_1, M^{-1} (UV)	K_1, M^{-1} (d−d)	K_1, M^{-1} (mean)
Co	2.44×10^4	1.93×10^4	$(2.18 + 0.25) \times 10^4$
Ni	7.02×10^4	6.57×10^4	$(6.79 + 0.22) \times 10^4$
Cu	1.70×10^7	1.17×10^7	$(1.43 \pm 0.27) \times 10^7$

Titration of the system Cu^{2+}/Hamac and NaOH up to pH 7 led to $K_2 = (5.32 \pm 3.2) \times 10^5$ M^{-1} for the formation of the bis complex Cu(amac)$_2$. In the case of cobalt and nickel, bis complex formation was not detectable.

Rate of Enolization/Ketonization and the Ratio [enol]/[ketone]. The rate constant k_e for enolization was determined by the bromination method described elsewhere.[3] The bromination of the enol is too fast to be monitored by the stopped-flow technique at ambient temperature. The stopped-flow spectrophotometric investigation of the reaction of Hamac with Br_2 at 452 nm ($\epsilon_{max}(Br_2)$ = 103 M^{-1} cm^{-1} [3]) led therefore to a sharp initial drop in absorbance, ΔA (=$A_{init} - A_0$), followed by a first-order decay of A from A_0 to A_∞. This first-order reaction, which corresponds to the enolization of the keto tautomer initially present, was studied at $[\text{Hamac}]_0 = [Br_2]_0 = 2.5 \times 10^{-3}$ M in the pH range 0.80−1.68 (I = 0.5 M, $NaClO_4$). The absorbance/time data were computer-fitted to eq 4, to obtain the parameters k_e, A_0, and A_∞ (Table 1).

$$A = (A_0 - A_\infty)\exp(-k_e t) + A_\infty \qquad (4)$$

Rate constant k_e is pH-independent and averages to $k_e = 0.0172 \pm 0.0004$ s^{-1} at 25 °C. The ratio [enol]/[ketone], following from the ratio of amplitudes (see Table 1), averages to 2.4 ± 0.1.

The rate constant of ketonization, k_k, was also determined by stopped-flow spectrophotometry. A solution of Hamac at pH 8.5, containing exclusively the enolate, was reacted with dilute $HClO_4$ to produce

(19) Elias, H.; Wiegand, D.; Wannowius, K. J. *Inorg. Chim. Acta* **1992**, *197*, 21.
(20) Abbreviations: Hamac = 3-(*N*-acetylamido)pentane-2,4-dione; HMOPS = 3-(*N*-morpholino)propanesulfonic acid; HMES = 2-(*N*-morpholino)-ethanesulfonic acid; HLUS = 2,6-dimethylpyridine-3-sulfonic acid; Hacac = acetylacetone = pentane-2,4-dione; Htfpd = 1,1,1-trifluoropentane-2,4-dione; Hhptd = heptane-3,5-dione; Htftbd = 4,4,4-trifluoro-1-(2-thienyl)butane-1,3-dione.
(21) Fackler, J. P., Jr.; Cotton, F. A. *Inorg. Chem.* **1963**, *2*, 102.
(22) Bips, U.; Elias, H.; Hauröder, M.; Kleinhans, G.; Pfeifer, S.; Wannowius, K. J. *Inorg. Chem.* **1983**, *22*, 3862.
(23) Wolff, L.; Bock, P.; Lorentz, G.; Trappe, P. *Liebigs Ann. Chem.* **1902**, *325*, 139.
(24) Elias, H.; Fröhn, U.; von Irmer, A.; Wannowius, K. J. *Inorg. Chem.* **1980**, *19*, 869.
(25) Drexler, C.; Elias, H.; Fecher, B.; Wannowius, K. J. *Fresenius J. Anal. Chem.* **1991**, *340*, 605.
(26) Stepwise titration with NaOH changes the pH, from which the degree of protonation, $n = [\text{Hamac}]/[\text{Hamac}]_0$, was calculated. Computer-fitting of the $n/[H^+]$ data[22] to $n = ([H^+]/K_a)/(1 + [H^+]/K_a)$ led to K_a.
(27) The species Hamac and amac$^-$ differ in their UV absorption. Stepwise titration with NaOH led to $A/[H^+]$ data (A = absorbance), which were computer-fitted to $A = [A_0(\text{Hamac}) + A_0(\text{amac}^-)K_a/[H^+]]/(1 + K_a/[H^+])$. The symbols A_0(Hamac) and A_0(amac$^-$) stand for the absorbance of the species Hamac and amac$^-$ at $[\text{Hamac}]_0$.
(28) The absorbance/$[H^+]$ data were fitted to eq I (monitoring in the UV range) or eq II

$$A = (A_0^{HL} + A_0^{ML}K_1[M^{2+}]_0K_a/[H^+])/(1 + K_1[M^{2+}]_0K_a/[H^+]) \qquad (I)$$

$$A = (A_0^{M} + A_0^{ML}K_1[HL]_0K_a/[H^+])/(1 + K_1[HL]_0K_a/[H^+]) \qquad (II)$$

(monitoring in the d−d range) with A_0^{HL}, A_0^{ML}, and A_0^{M} being the absorbance of the species HL, ML, and M at concentrations $[M^{2+}]_0$ (eq I) and $[HL]_0$ (eq II), respectively.

Table 1. Rate Constants for the Enolization and Ketonization of Hamac at 298 K ($I = 0.5$ M)

pH	k_e, s^{-1} [a]	$(k_e + k_k)$, s^{-1} [b]	ΔA, %[c]	$A_0 - A_\infty$, %[c]	$\Delta A/(A_0 - A_\infty) =$ [enol]/[ketone]
0.80	0.0175		69.6	30.4	2.29
1.06	0.0167		70.9	29.1	2.44
1.68	0.0175		71.2	28.8	2.47
1.09		0.0247			
1.45		0.0240			
2.34		0.0240			
3.02		0.0256			

[a] Obtained by fitting the A/t data to eq 4; $[\text{Hamac}]_0 = [\text{Br}_2]_0 = 2.5 \times 10^{-3}$ M. [b] Obtained by fitting the A/t data to eq 5; $[\text{Hamac}]_0 = 5 \times 10^{-5}$ M. [c] The parameters ΔA and $(A_0 - A_\infty)$ are described in the Experimental Section.

Table 2. Crystallographic Data for $Cu(amac)_2$·toluene

$C_{21}H_{28}CuN_2O_6$	$Z = 8$
fw = 467.98	$T = 26.0$ °C
space group: $C2/c$ (No. 15)	$\lambda = 0.710\ 69$ Å
$a = 20.434(6)$ Å	$\rho(\text{calcd}) = 1.38$ g cm^{-3}
$b = 11.674\ (4)$ Å	$\mu = 10.0$ cm^{-1}
$c = 19.278\ (6)$ Å	$R(F_o)^a = 0.0742$
$\beta = 100.75(1)°$	$R_w(F_o)^b = 0.0596$
$V = 4517.85 \pm 4.2$ Å^3	

[a] $R(F_o) = \sum|F_o - F_c|/\sum F_o$. [b] $R_w(F_o) = \sum w^{1/2}|F_o - F_c|/w^{1/2}\sum F_o$.

exclusively the enol. The ketonization of the enol, which is a reversible first-order reaction with $k_{obsd} = k_e + k_k$, was followed at different pH values ($I = 0.5$ M, $NaClO_4$). The A/t data were fitted to eq 5 to obtain

$$A = (A_0 - A_{eq}) \exp[-(k_e + k_k)t] + A_{eq} \quad (5)$$

the pH-independent sum of k_e and k_k (Table 1). The averaged values of $(k_e + k_k) = 0.0246 \pm 0.0015$ s^{-1} and $k_e = 0.0172$ s^{-1} (see above) led to $k_k = 0.0074 \pm 0.0015$ s^{-1} at 25 °C.

Kinetics of Complex Formation. Reaction 3 was followed by stopped-flow or rapid-scan-stopped-flow spectrophotometry at $I = 0.5$ M ($NaClO_4$) and variable pH in buffered solution under pseudo-first-order conditions ($[M^{2+}]_0 \geq 10[\text{Hamac}]_0$). The A/t data, resulting from the increase in absorbance at 300−315 nm with time, were computer-fitted to eq 6 (irreversible biphasic consecutive reaction). The fitting

$$A = a_f[\exp(-k_f t)] + a_s[\exp(-k_s t)] + A_\infty \quad (6)$$

procedure, based on the least-squares method, led to a_f, a_s, A_∞, k_f, and k_s (k_f, k_s = rate constants for the fast and slow reaction; a_f, a_s = corresponding amplitudes in units of absorbance).

Kinetics of Acid Hydrolysis. Reaction 7 was followed as described for complex formation according to (3), with $HClO_4$ being the excess

$$M(amac)^+ + H^+ \rightarrow M^{2+} + \text{Hamac} \quad (7)$$

partner ($[HClO_4]_0 \geq 10[M(amac)^+]_0$). The A/t data of the biphasic process were computer-fitted with eq 6.

X-ray Structure Determination. The green crystal of $Cu(amac)_2$·toluene, as grown from the ethanol/toluene reaction mixture, was needle-shaped and had the dimensions 0.15 × 0.16 × 1.2 mm. Intensities were measured on a four-circle diffractometer (Stoe-Stadi-4) using graphite-monochromatized Mo Kα radiation ($\lambda = 0.710\ 69$ Å; scan $2\theta{:}\omega = 1{:}1$). Cell constants were determined by the least-squares method from the 2θ angles of 94 reflections ($T = 299$ K) on the same instrument. *Lp* and background corrections and a numerical absorption correction (EMPIR and REDU4 (Stoe); $T_{min} = 0.935$ and $T_{max} = 1.000$) were applied.

The structure was solved by direct methods with SHELXS-86 (PATT) and refined by least-squares to the R values given in Table 2. Hydrogen atoms were positioned geometrically (C−H distance = 0.96 Å) and not refined. An empirical extinction correction was applied. All crystallographic calculations were performed with the programs SHELX-76 and SHELXS-86 on an IBM 3090 computer at the Technische Hochschule Darmstadt. Scattering factors f_0, f', and f'' for C, H, N, and O are stored in SHELX-76.[29] The final positional parameters are given in Table 3.

Table 3. Atomic Parameters ($\times 10^4$) for $Cu(amac)_2$·toluene (Excluding H)

atom	x/a	y/b	z/c	U_{eq}, Å^2 [a]
Cu1	4846(1)	4721(1)	4150(1)	417(5)
O1	4209(2)	5911(5)	3991(2)	473(31)
C1	3250(4)	6987(7)	3525(5)	785(56)
C2	3628(4)	5854(7)	3646(3)	472(40)
C3	3301(3)	4849(7)	3361(3)	412(39)
C4	3617(4)	3776(7)	3450(3)	463(43)
C5	3237(4)	2728(7)	3123(5)	741(54)
O2	4206(2)	3586(4)	3776(2)	498(31)
N1	2638(3)	4931(6)	2964(3)	467(35)
C6	2093(3)	4816(7)	3270(4)	516(44)
O3	2118(3)	4752(6)	3895(2)	821(38)
C7	1438(3)	4797(8)	2739(4)	714(49)
O4	5517(2)	3567(4)	4232(2)	492(31)
C8	6539(4)	2648(7)	4320(4)	663(51)
C9	6150(4)	3714(7)	4377(3)	417(42)
C10	6451(3)	4766(8)	4541(3)	400(38)
C11	6120(3)	5769(7)	4616(3)	426(42)
C12	6478(4)	6884(7)	4784(4)	662(50)
O5	5481(2)	5849(4)	4553(2)	512(31)
N2	7170(3)	4826(6)	4672(3)	449(34)
C13	7528(4)	4899(7)	4160(4)	481(43)
O6	7285(2)	4838(6)	3535(2)	682(35)
C14	8268(3)	5051(7)	4417(3)	508(43)

[a] $U_{eq} = {}^1/_3\sum_i\sum_j \mathbf{U}_{ij} a_i^* a_j^* a_i a_j$.

Results

The β-Diketone Hamac. Hamac is a colorless solid which, due to the polar acetamido group in 3-position, is well soluble in water. The solubility (2.45 M) exceeds that of Hacac by a factor of 1.5. Moreover, the complex $Cu(amac)_2$ can be dissolved in water up to 0.56 M, which is 700 times higher than for $Cu(acac)_2$. The pK_a of Hamac, as determined independently by potentiometric and spectrophotometric titration, is 7.01 ± 0.07 (mean of 7.08 and 6.93). Hamac is thus by almost two pK units more acidic than Hacac (see Table 4).

The rate of enolization of Hamac ($k_e = 0.0172$ s^{-1}) is rather close to that of Hacac and Htfpd[20] ($k_e = 0.015$ s^{-1}), but the rate of ketonization is considerably smaller (Table 4). This means that the enol/ketone equilibrium is much more shifted toward the enol tautomer, with $K = k_e/k_k = 2.3 \pm 0.4$. The spectrophotometric investigation of the kinetics of enolization according to the bromination method leads to the reaction amplitudes ΔA and $(A_0 - A_\infty)$, the ratio of which corresponds to K (see Table 1). This independently obtained value amounts to $K = 2.4 \pm 0.1$ and is in good agreement with the value following from the ratio k_e/k_k. To our knowledge, the ligand Hamac is thus the most strongly enolized β-diketone so far studied kinetically.

Structure of the Complex $Cu(amac)_2$·toluene. The ligand Hamac carries three donor oxygen atoms in total so that the question of O(acetyl) coordination cannot be excluded. It follows from Figure 1, however, that in the complex unit $Cu(amac)_2$ the ligand prefers the normal coordination with the two β-diketone oxygens being bound to the copper. The complex is centrosymmetric and crystallizes in the monoclinic space group $C2/c$ with 8 formula units per unit cell. Half of the toluene is located on a 2-fold axis; the other half is located close

(29) Data for Cu was taken from: *International Tables for X-ray Crystallography*; Kynoch Press: Birmingham, England, 1974, Vol. IV.
(30) Pearson, R. G.; Moore, J. W. *Inorg. Chem.* **1966**, *5*, 1528.

Table 4. Parameters Characterizing the β-Diketone Hamac[a]

β-diketone[20]	solubility, M	pK_a	k_e, s^{-1}	k_k, s^{-1}	$K = k_e/k_k$ = [enol]/[ketone]	ref
Hamac	2.45	7.01 ± 0.07	0.0172 ± 0.0004	0.0074 ± 0.0015	2.3 ± 0.4 2.4 ± 0.1[b]	this work
Hacac	1.6	9.00	0.015	0.114	0.13	30
Htfpd		6.06	0.015	1.5	0.01	10
Hhptd		10.0	0.0058	0.048	0.12	7

[a] The data refer to the solvent water, I = 0.5 M, and 298 K. [b] As determined from the ratio of amplitudes (see Table 1).

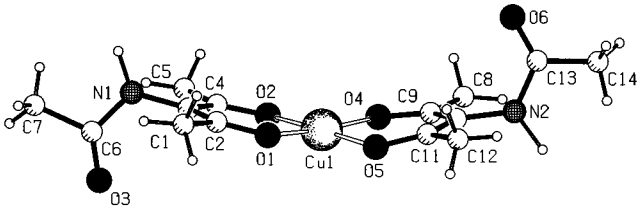

Figure 1. View of the coordination geometry in the complex $Cu(amac)_2$.

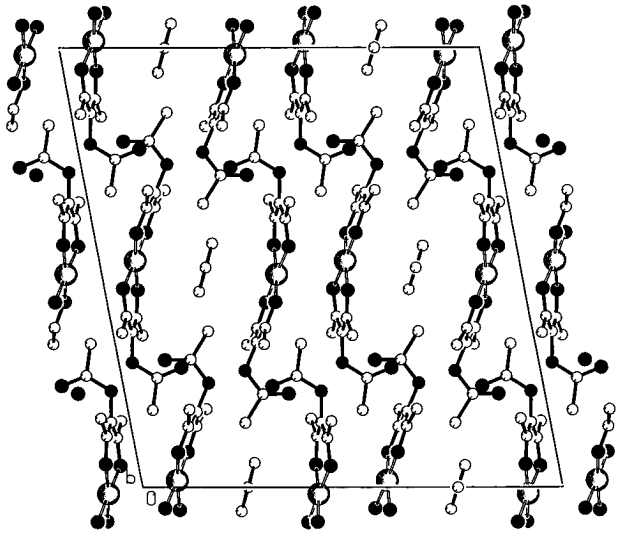

Figure 2. Projection of the unit cell of the complex $Cu(amac)_2$·toluene along [010].

to a center of symmetry and is highly disordered, which limited the refinement to R_w = 0.0596 (Table 2).

The copper coordinates the two ligands in a planar fashion. The planes of the two chelate rings are slightly bent off the CuO_4 coordination plane though, with the two *N*-acetylamido groups pointing into opposite directions (Figure 1). As shown in Figure 2, the units of $Cu(amac)_2$ form dimers (Cu−Cu distance = 329 pm; shortest intermolecular Cu−O distance = 279 pm). The dimeric units are stabilized by weak intermolecular hydrogen bonds between N2 and O3 (distance = 291 pm) and the dimers are stacked along [001] via weak hydrogen bonds between N1 and O6 (distance = 292 pm). The toluene located on the twofold axis is sitting between the stacked dimers. The Cu−Cu distance of 329 pm and the normal magnetic moment of 1.93 μ_B point to the absence of metal−metal interactions. The planar arrangement of the CuO_4 coordination core is slighly distorted (see angles and distances in Table 5). The average Cu−O distance (190.3 pm), C−O distance (127.3 pm), and C−C distance within the chelate rings (139.3 pm; see Table 5) is rather close to what is found for similar β-diketone copper complexes of the type bis(3-*R*-pentane-2,4-dionato)-copper(II) with R = phenyl[31] or methyl.[32] The C−C and C−O

Table 5. Selected Distances (pm) and Bond Angles (deg) for $Cu(amac)_2$·toluene

	Distances		
Cu−O1	188.9(5)	C1−C2	152.8(10)
Cu−O2	190.6(5)	C4−C5	152.1(10)
Cu−O4	190.7(5)	C8−C9	149.3(10)
Cu−O5	191.1(5)	C11−C12	149.8(10)
O1−C2	124.9(8)	C3−N1	142.7(8)
O2−C4	126.9(8)	C10−N2	144.5(8)
O4−C9	128.3(8)	N1−C6	135.6(9)
O5−C11	129.1(8)	N2−C13	133.6(8)
C2−C3	141.0(10)	C6−C7	152.6(9)
C3−C4	140.4(10)	C13−C14	151.1(9)
C9−C10	138.3(10)	C6−C3	120.0(8)
C10−C11	137.3(10)	C13−O6	121.8(8)
		Cu−Cu[a]	328.6(2)
	Angles		
O1−Cu−O2	92.7(2)	O4−Cu−O5	91.7(2)
Cu−O2−C4	125.9(5)	Cu−O4−C9	127.1(5)
Cu−O1−C2	127.2(5)	Cu−O5−C11	125.9(5)
O2−C4−C3	126.0(7)	O4−C9−C10	123.8(7)
O1−C2−C3	125.9(7)	O5−C11−C10	124.1(7)
C2−C3−C4	121.4(6)	C9−C10−C11	125.0(6)

[a] Distance between neighboring complex units.

distances lie in between those for single and double bonds and reflect delocalization of electron density within the chelate rings formed, which is typical for β-diketone complexes.

Kinetics of Complex Formation. The reaction of Hamac with an excess of the divalent metal ions M^{2+} (M = Co, Ni, Cu) leads to the species $M(amac)^+$. These species absorb strongly in the UV and have weak d−d transitions in the visible range (see Experimental Section). The strong absorption at about 300 nm corresponds to the $\pi \rightarrow \pi^*$ transition of the enolate $amac^-$, which is bathochromically shifted and intensified upon coordination to the metal. Monitoring of the formation of the species $M(amac)^+$ at 300−315 nm should therefore result in an increase in absorbance.

As an example, Figure 3a shows the series of spectra obtained for the reaction of an excess of Ni^{2+} ions with Hamac at pH 6.2. The first 50 spectra were recorded every second, the second set of 50 spectra every 5 s. The reaction is obviously biphasic. As shown in Figure 3b, the first set of spectra is characterized by a sharp isosbestic point at 288 nm, with a decrease in absorbance below 288 nm and an increase above. This initial reaction step is followed by a slower reaction (see Figure 3c), associated with a gradual increase of the absorption peak at 302 nm, typical for $Ni(amac)^+$. The A/t data can be fitted to the sum of two exponentials (eq 6), which leads to rate constants k_f (fast initial step) and k_s (slower second step). For M = Co, Cu the same type of biphasic kinetics is observed.

Variation of $[M^{2+}]_0$ at constant pH leads to the data summarized in Table 6. Rate constant k_f increases with increasing $[M^{2+}]_0$ and, for a given concentration of the metal, its size depends on the nature of the metal according to $k_f(Cu) > k_f(Co) > k_f(Ni)$. Rate constant k_s is independent of $[M^{2+}]_0$, nearly of the same size for M = Ni, Co and somewhat larger for M = Cu. These findings suggest that the k_r step describes complex formation and that the k_s step has to do with the

(31) Carmichael, J. W., Jr.; Steinrauf, L. K.; Belford, R. L. *J. Chem. Phys.* **1965**, *43*, 3959.
(32) Robertson, J.; Truter, M. R. *J. Chem. Soc. A* **1967**, 309.

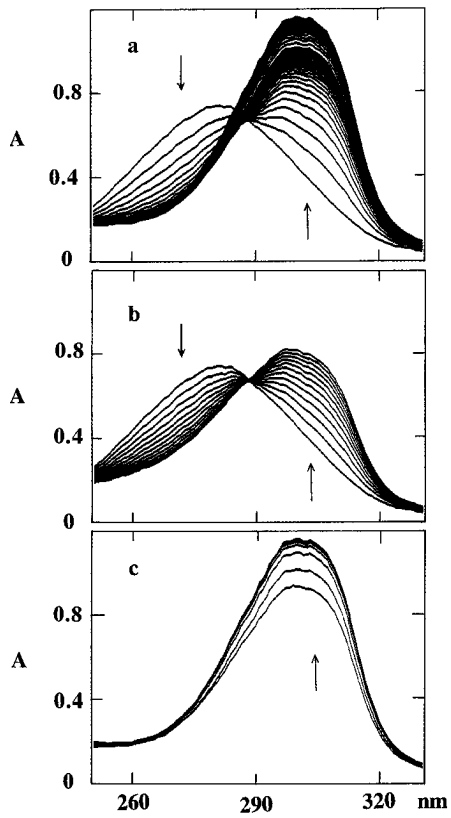

Figure 3. Spectral changes in the UV range associated with the reaction of Ni^{2+} ions ($[Ni^{2+}]_0 = 5 \times 10^{-3}$ M) with Hamac ($[Hamac]_0 = 5 \times 10^{-5}$ M) in water at pH 6.2, 298 K, and $I = 0.5$ M ($NaClO_4$) Key: (a) 100 consecutive spectra, with $\Delta t = 1$ s for spectra 1−50 and $\Delta t = 5$ s for spectra 51−100 (every second spectrum omitted for clarity); (b) spectra 1−12; (c) spectra 25, 50, 60, 70, 80, 90, and 100.

Table 6. Rate Constants k_f and k_s for the Reaction of Hamac with Ni^{2+}, Cu^{2+}, and Co^{2+} Ions According to Eq 3 at 298 K[a,b]

$[M^{2+}]$, mM	pH[c]	k_f, s^{-1}	k_s, s^{-1}
	M = Ni		
0.50	4.94	0.0485	0.0104
1.25	4.87	0.0654	0.0231
2.50	4.85	0.0850	0.0237
3.75	4.84	0.104	0.0249
5.00	4.84	0.121	0.0243
12.5	4.85	0.233	0.0246
25.0	4.83	0.396	0.0248
	M = Cu		
0.050	3.49	18.2	0.144
0.125	3.47	20.3	0.162
0.250	3.48	23.7	0.154
0.500	3.47	28.8	0.150
1.00	3.47	42.7	0.138
2.00	3.45	64.7	0.128
	M = Co		
0.50	4.89		0.0066
1.25	4.87	8.67	0.0115
2.50	4.84	9.70	0.0237
3.75	4.86	10.1	0.0238
5.00	4.83	11.2	0.0255
12.5	4.81	15.7	0.0259
25.0	4.80	23.4	0.0265

[a] Conditions $[Hamac]_0 = 5 \times 10^{-5}$ M; $I = 0.5$ M ($NaClO_4$). [b] k_f and k_s obtained by computer-fitting of the *A*/*t* data to eq 6. [c] The pH was adjusted with the buffers HLUS[20] (Ni, Co) and formic acid (Cu) at [buffer] = 0.1 M.

tautomerism of the liand Hamac. Convincing support for this interpretation comes from two experiments. In the first one, excess Ni^{2+} ions were reacted exclusively with the enol tautomer of Hamac at pH 5.5.[33] The *A*/*t* data thus obtained could be well fitted to a single exponential according to (4); i.e. only one step was observed. The first-order rate constant resulting from this experiment increases with increasing $[Ni^{2+}]_0$ (Table 7), as does k_f. This result indicates that the k_s step obviously describes the (slow) enolization of the keto tautomer of Hamac after the enol tautomer has been consumed in (fast) complex formation with the nickel present in excess. In addition, the fact that $k_s \neq f([Ni]_0)$ is consistent with the interpretation that the keto tautomer as such does not add to the nickel. The second experiment concerns the reaction of Co^{2+} ions with an excess of Hamac, as monitored in the d−d range. In this case the *A*/*t* data could also be fitted to a single exponential according to (4). The resulting first-order rate constant increases with increasing $[Hamac]_0$ (Table 7). These findings suggest that, for $[Hamac]_0 \geq 10[Co^{2+}]_0$, there is an excess of enolic Hamac present to completely convert the Co^{2+} ions into the species $Co(amac)^+$ in a pseudo-first-order reaction.

Table 7. First-Order Rate Constant for the Reaction of Ni^{2+} Ions with Exclusively the Enol Tautomer of Hamac[33] and for the Reaction of Co^{2+} Ions with an Excess of Hamac at 298 K ($I = 0.5$ M)

$[Ni^{2+}]$, mM[a]	pH[b]	k, s^{-1} [c]	[Hamac], M[d]	pH[e]	k, s^{-1} [f]
1.00	5.50	0.0831	0.0375	4.65	21.4
2.50	5.51	0.116	0.050	4.67	25.2
5.00	5.51	0.179	0.075	4.60	35.3
10.0	5.43	0.295	0.10	4.61	43.4
25.0	5.45	0.660	0.15	4.55	51.8
50.0	5.50	1.26			

[a] $[Hamac]_0 = 5 \times 10^{-5}$ M. [b] Adjusted with HMES. [c] Obtained by fitting eq 4 to the *A*/*t* data recorded at 300 nm. [d] $[Co^{2+}]_0 = 0.00375$ M. [e] Adjusted with HLUS. [f] Obtained by fitting eq 4 to the *A*/*t* data recorded at 500 nm.

The reaction of Hamac with copper is much faster than that with nickel and cobalt. For experimental reasons the concentration of excess copper had therefore to be kept low. As shown in Table 6, for some of the copper experiments the pseudo-first-order condition ($[Cu^{2+}]_0 \geq 10[Hamac]_0$) was not fulfilled. The surprising result was however that even for $[Cu^{2+}]_0$:$[Hamac]_0$ = 1:1 and 2.5:1 the *A*/*t* data could be well fitted to eq 6.[34] A simple interpretation of this finding would come from the assumption that the species $Cu(amac)^+$ is mainly formed via the reaction of the Cu^{2+} ion with the enolate $amac^-$, for which the condition $[Cu^{2+}]_0 \gg [amac^-]$ is of course fulfilled in the pH range 3−4.7.

Figure 4 shows the plot of the dependence $k_f = f([Ni^{2+}]_0)$ and $k_s = f([Ni^{2+}])$, respectively, for the system Ni^{2+}/Hamac at three different pH values. The rate constant k_s for the slower second reaction step is independent of $[Ni^{2+}]_0$ (Figure 4b) and increases weakly with increasing pH. The averaged size of k_s is close to that of the rate constant for the enolization of Hamac, $k_e = 0.0172$ s^{-1} (Table 4), but is somewhat larger. An explanation for this comes from the study of the rate of enolization at variable pH in the presence of buffers.[35] This study shows that the enolization of Hamac is subject to general base catalysis. Hydroxyl ions and the B^- ions of added buffers HB affect k_e according to $k_e = k_{HOH}[H_2O] + k_{OH}[OH^-] + k_B[B^-]$. The term $k_{HOH}[H_2O]$ amounts to 0.017 ± 0.001 s^{-1} at

(33) The solution of Hamac used for this stopped-flow experiment was set to pH 8.4 to convert Hamac completely to $amac^-$. This solution was reacted with solutions of nickel perchlorate of pH 5.5 (as adjusted with the buffer HMES[20]) to produce reaction mixtures of pH 5.5 containing only the enol tautomer of Hamac upon mixing.

(34) In the case of the experiment with the stoichiometry $[Cu^{2+}]_0$:$[Hamac]_0$ = 1:1 it was attempted to fit the *A*/*t* data for the fast initial step to the equation valid for a 1:1 second-order reaction, $A = A_\infty + (A_0 - A_\infty)/(1 + [Cu^{2+}]_0 kt)$. The quality of the fit was very poor though.

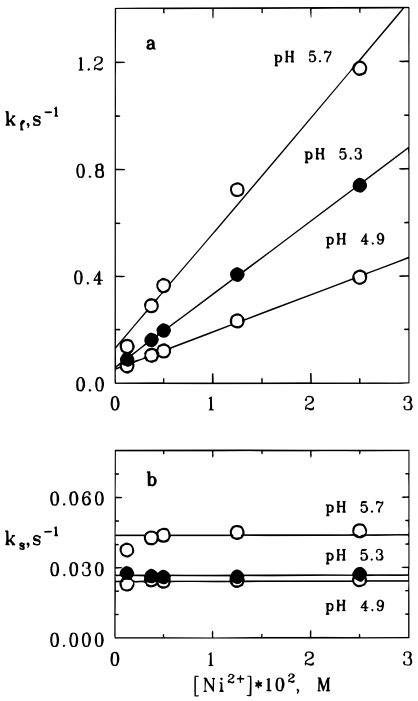

Figure 4. Plot of the experimental rate constants k_f and k_s vs the concentration of nickel ions for reaction 3 at variable pH and 298 K ($[Hamac]_0 = 5 \times 10^{-5}$M).

298 K, and the increase in k_s with increasing pH and with different buffers (see Figure 4b) is thus due to increasing base catalysis.

As shown in Figure 4a for M = Ni, the experimental rate constant k_f, describing the formation of the mono complex $M(amac)^+$, increases linearly with $[M^{2+}]_0$ at a given pH according to (8). Fittings of eq 8 to the $k_f/[M^{2+}]_0$ data leads to rate constants k_0 and k_2, as summarized in Table 8.

$$k_f = k_0 + k_2[M^{2+}]_0 \quad (8)$$

The size of k_2 is pH-dependent (see Figure 4a). If, according to Scheme 1, complex formation takes place with enolic Hamac (=HE) as well as with the enolate amac$^-$ (=E$^-$), the rate of complex formation should follow eq 9 (in view of the excess

$$d[ME^+]/dt = k_{HE}[HE][M^{2+}]_0 - k_{-HE}(K_{MEH})^{-1}[ME^+][H^+] + k_E[E^-][M^{2+}]_0 \quad (9)$$

condition, $[M^{2+}]_0 \gg [Hamac]_0$, the reverse reaction, as characterized by the rate constant k_{-E}, is neglected).[37] Integration of (9) leads to an exponential with an experimental rate constant, $k_{obsd} \equiv k_f$, as described by eq 10. For a given pH (i.e., $[H^+] =$

$$k_f = k_{-HE}(K_{MEH})^{-1}[H^+] + (k_{HE} + k_E K_a/[H^+])(1 + K_a/[H^+])^{-1}[M^{2+}]_0 \quad (10)$$

constant), eq 10 corresponds to eq 8 with $k_0 = k_{-HE}(K_{MEH})^{-1}[H^+]$ and $k_2 = (k_{HE} + k_E K_a/[H^+])/(1 + K_a/[H^+])$. The plot of $k_2(1 + K_a/H^+)$ vs $K_a/[H^+]$ according to (11) should therefore give a

$$k_2(1 + K_a/[H^+]) = k_{HE} + k_E K_a/[H^+] \quad (11)$$

linear dependence with a slope of k_E and an intercept k_{HE}. Figure 5 shows this type of plot for M = Ni, Cu, and Co and

Table 8. Rate Constants k_2, k_0, and k_s for the Formation of the Species $M(amac)^+$ According to Eq 3 at Variable pH, 298 K, and I = 0.5 M[a]

pH[b]	k_2, M^{-1} s^{-1} [c]	k_0, s^{-1} [d]	k_s, s^{-1} [c]
	M = Ni		
4.8	14.2	0.049	0.0242
5.3	27.4	0.058	0.0268
5.5	47.0[e]	0.056[e]	
5.7	43.4	0.119	0.0439
6.0	79.1	0.082	0.0578
6.2	100	0.144	0.0743
6.4	164	0.089	0.0846
6.7	253	0.189	0.109
7.0	418	0.177	0.155
7.7	659	0.738	0.518
	M = Cu		
3.0	17 000	23.7	0.0904
3.5	24 000	17.4	0.146
4.3	150 000	11.0	0.0222
4.7	309 000	5.67	0.0248
	M = Co		
4.6	275[f]	12.6[f]	
4.9	618	7.89	0.0251
5.3	1510	7.59	0.0298
5.6	1920	6.99	0.0465
6.0	6050	3.11	0.0656
6.2	8060	10.0	0.0809

[a] Each set of rate constants k_2, k_0, and k_s at a given pH is based on a series of stopped-flow experiments at five to seven different concentrations of excess M^{2+} ions at $[Hamac]_0 = 5 \times 10^{-5}$M (as shown, for example, in Table 6), leading to five to seven pairs of rate constants k_f and k_s at the given pH. Fitting of the k_f data to eq 8 for a given pH leads to rate constants k_2 and k_0. [b] As adjusted with the buffers formic acid (pH 3.0−3.5), HLUS[20] (pH 4.3−5.3), HMES[20] (pH 5.5−6.7), and HMOPS[20] (pH 7.0−7.7). [c] The error limits for k_2 and k_s are of the order ±5%. [d] Due to the fact that k_0(=intercept) is determined by extrapolation the error limits for k_0 are very high. This is especially true for "steep" dependencies, i.e. for large k_2 values. [e] Experiment with exclusively the enol tautomer of Hamac (see Table 7).[33] [f] Experiment with an excess of Hamac (see Table 7).

Scheme 1. Schematic Description of the Various Steps Controlling the Formation and Acid Dissociation of the Species $M(amac)^+ = ME^+$

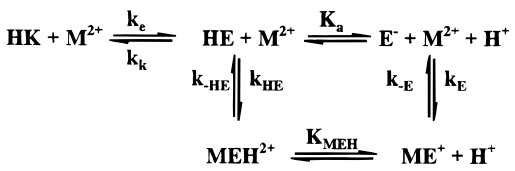

Table 9 presents the data for k_{HE} and k_E, as obtained by computer-fitting.

Table 10 presents the temperature dependence of rate constants k_f and k_s and the corresponding activation enthalpies $\Delta H^{\ddagger}$. These activation enthalpies are not pure activation parameters since both k_f and k_s are not single rate constants but are instead composite experimental parameters.

(35) The rate law for the enolization of the keto tautomer HK of Hamac at variable pH in the presence of buffers HB was found to be a three-term rate law, $v = (k_{HOH}[H_2O] + k_{OH}[OH^-] + k_B[B^-])[HK]$, with $k_{HOH} = (3.07 \pm 0.09) \times 10^{-4}$ M^{-1} s^{-1}, $k_{OH} = (1.5 \pm 0.1) \times 10^5$ M^{-1} s^{-1}, and k_B on the order of 1 M^{-1} s^{-1} for the buffers HMES and HMOPS.[36] In the absence of buffers and at pH < 4.8, the rate is given by $v = k_{HOH}[H_2O][HK]$.

(36) Dr. Ing. Thesis, submitted to Technische Hochschule Darmstadt (D17) by J.H. in 1994.

(37) The equilibrium $MEH^{2+} \rightleftharpoons ME^+ + H^+$ is a fast equilibrium. At pH > pK_{MEH} the formation of the species MEH^{2+} corresponds therefore to the formation of the species ME^+.

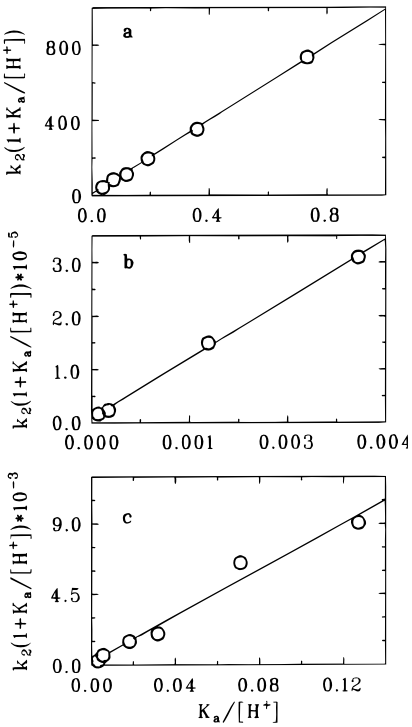

Figure 5. Plot of the term $k_2(1 + K_a/[H^+])$ vs $K_a/[H^+]$ according to eq 11 for nickel (a), copper (b), and cobalt (c).

Table 9. Rate and Equilibrium Constants for the Formation and Acid Dissociation of the Species M(amac)$^+$ (M = Ni, Co, Cu) at 298 K and I = 0.5 M ($NaClO_4$)

	M = Ni	M = Co	M = Cu
k_{HE}, M^{-1} s^{-1}	18 ± 6	180 ± 350	(9 ± 5) × 10^4
			(1.3 ± 0.7) × 10^4 [a]
k_E, M^{-1} s^{-1}	924 ± 6	(7.4 ± 0.6) × 10^4	(8.4 ± 0.2) × 10^8
k_{OH}, M^{-1} s^{-1}			(3.0 ± 0.1) × 10^8 [a]
k_{-HE}, s^{-1}	≥10.3[b]	240 ± 43	1330 ± 210
k_{-E}, s^{-1}	0.054 ± 0.005	9.5 ± 2.3	15.7 ± 1.6
K_{MEH}, M	≥0.5[b]	0.0038 ± 0.0013	0.22 ± 0.05
k_E/k_{-E}, M^{-1}	1.7 × 10^4	0.91 × 10^4	5.4 × 10^7
K_1, M^{-1} [c]	6.79 × 10^4	2.18 × 10^4	1.6 × 10^7
k_{ex}, s^{-1} [d]	3.2 × 10^4	3.2 × 10^6	4.4 × 10^9
$k_{i,E}/k_{ex}$ [e]	0.048	0.039	0.32
$k_{i,HE}/k_{ex}$ [f]	1.9 × 10^{-3}	1.9 × 10^{-4}	6.8 × 10^{-5}

[a] As obtained by fitting eq 16b to the $k_2/[H^+]$ data. [b] Estimated on the basis of the condition $[H^+]/K_{MEH} \leq 0.1$. [c] Spectrophotometrically determined formation constant for the species M(amac)$^+$ according to eq 3a. [d] Rate constant for water exchange at 298 K.[44,45] [e] Calculated on the basis of $k_{i,E} = k_E/K_{OS}$ for k_{OS} = 0.6 M^{-1}.[46] [f] Calculated on the basis of $k_{i,HE} = k_{HE}/K_{OS}$ for K_{OS} = 0.3 M^{-1}.[46]

Kinetics of Acid Hydrolysis. The acid hydrolysis of the mono complex M(amac)$^+$ (M = Co, Ni, Cu), as monitored spectrophotometrically in the UV range, was found to be a three-step process. The first step is a sharp change in absorbance, ΔA, too fast to be monitored by the stopped-flow technique. This initial rapid step is followed by a change in absorbance with time to which eq 6 can be fitted satisfyingly. The fitting procedure leads to first-order rate constants k_f for a fast second step and k_s for a third slower step (see Table 11). The rate cosntant k_s is pH-independent and found to the same for M = Co, Ni, and Cu; its size corresponds to ($k_e + k_k$) (see Table 1). This means that the k_s step is indeed the final third step describing the ketonization of enolic Hamac liberated by the acid hydrolysis of the species M(amac)$^+$.

The very rapid initial change in absorbance, ΔA, increases with decreasing pH. It is therefore suggested that, according to Scheme 1, the first step consists in the fast protonation of the complex M(amac)$^+$ = ME$^+$. The concentration of the species MEH^{2+} thus formed is governed by the pH. The decay of ME$^+$ and MEH^{2+} liberates the enol HE (second step; k_f), which finally ketonizes (third step; $k_s = k_e + k_k$). If so, the experimental rate constant k_f for the observable fast step of acid hydrolysis should follow relationship 12. The plot of $k_f = f$(pH)

$$k_f = (k_{-E} + k_{-HE}[H^+]/K_{MEH})/(1 + [H^+]/K_{MEH}) \quad (12)$$

for M = Co, as shown in Figure 6, indicates the expected saturation type behavior of k_f.[38] Computer-fitting of eq 12 to the data leads to the parameters k_{-E}, k_{-HE} and K_{MEH} for M = Co and Cu, albeit with large errors for k_{-HE} and K_{MEH} (see Table 9). In the case of nickel the dependence of k_f on $[H^+]$ is linear up to pH 1.3. A linear dependence of k_f on $[H^+]$ follows from eq 12 for the condition $[H^+]/K_{MEH} \leq 0.1$. This in turn means for pH 1.3 that the condition $K_{MEH} \geq 0.5$ has to be fulfilled. It follows from the numbers obtained for K_{MEH} that, compared to the complex cation Co(amac)$^+$, the species Ni(amac)$^+$ and Cu(amac)$^+$ are only weakly protonated.

Table 10. Temperature Dependence of Rate Constants k_f and k_s for the Formation of the Species M(amac)$^+$ According to Eq 3 at I = 0.5 M and Activation Parameter $\Delta H^{\ddagger}$

	M = Ni[a]		M = Co[b]		M = Cu[c]	
T, K	k_f, s^{-1}	k_s, s^{-1}	k_f, s^{-1}	k_s, s^{-1}	k_f, s^{-1}	k_s, s^{-1}
285	0.204	0.0297				
288	0.261	0.0325	12.9	0.0416	9.98	0.00739
291	0.353	0.0411				
293	0.439	0.0543	19.3	0.0594	13.6	0.0166
298	0.687	0.0703	29.0	0.0832	17.6	0.0241
303	1.08	0.0995	43.6	0.120	24.2	0.0366
308	1.60	0.136	60.3	0.164	29.2	0.0444
313	2.40	0.188	86.3	0.231	44.2	0.0605
$\Delta H^{\ddagger}$, kJ mol^{-1} [d]	63.4 ± 1	47.6 ± 2	54.7 ± 2	48.7 ± 1	40.6 ± 2	46.4 ± 3

[a] At pH 6.2 (buffer: HMES), $[Ni^{2+}]_0 = 0.005$ M, $[Hamac]_0 = 5 \times 10^{-5}$ M. [b] At pH 6.2 (buffer: HMES), $[Co^{2+}]_0 = 0.0025$ M, $[Hamac]_0 = 5 \times 10^{-5}$ M. [c] At pH 4.2 (buffer: HLUS), $[Cu^{2+}]_0 = [Hamac]_0 = 5 \times 10^{-5}$ M. [d] Obtained from the slope of the plot of $\ln(k_f/T)$ and $\ln(k_s/T)$, respectively, vs $1/T$. The data for $\Delta S^{\ddagger}$ are not presented. Due to the fact that both k_f (see eqs 10 and 12) and k_s (=k_e)[35] are composite parameters the data for $\Delta S^{\ddagger}$ are rather meaningless.

Discussion

In aqueous solution the ligand Hamac is present mainly in its enolic form (70%). In the complex Cu(amac)$_2$·toluene (see Figure 1) and, most probably, in all of the species M(amac)$^+$ studied the ligand behaves like an unsubstituted β-diketone and coordinates the metal via the two diketo oxygens. The kinetic results are consistent with the interpretation that the keto tautomer of Hamac does not add to the metal. The coordination of the enol tautomer, as studied with an excess of metal ion, is biphasic. There is a fast initial step (k_f), describing "fast" M(amac)$^+$ formation, and a slower consecutive step (k_s), describing "slow" M(amac)$^+$ formation, as controlled by the enolization of the "unreactive" keto tautomer. The rate of the latter process is subject to general base catalysis. The activation enthalpies $\Delta H^{\ddagger}$ for the slower second step (k_s) of the reaction with nickel, cobalt, and copper agree within the limits of error (see Table 10). This result supports the interpretation that the k_s step describes the enolization of the keto tautomer of Hamac. For a given pH, rate constant k_f for complex formation increases linearly with the metal concentration according to eq 8, which

(38) It would have been most desirable to extend the measurements to higher proton concentrations. This was however limited by the k_f step becoming too fast for observation.

Table 11. Experimental Rate Constants for the Acid Hydrolysis[a] of the Species M(amac)$^+$ at Variable pH, 298 K, and I = 0.5 M ($NaClO_4$)

M = Co[b]				M = Cu[c]				M = Ni[d]			
pH[e]	k_f, s^{-1} [f]	k_s, s^{-1} [f]	ΔA[g]	pH[e]	k_f, s^{-1} [f]	k_s, s^{-1} [f]	ΔA[g]	pH[e]	k_f, s^{-1} [f]	k_s, s^{-1} [f]	ΔA[g]
3.81	18.8	0.0283	0.054	2.86	22.9	0.0220	0.030	3.70	0.065	0.0194	0.017
3.56	24.7	0.0266	0.103	2.50	34.5	0.0236	0.114	2.63	0.101	0.0241	0.049
3.45	30.3	0.0258	0.079	2.27	47.9	0.0235	0.119	2.34	0.148	0.0252	0.045
3.12	45.1	0.0258	0.100	2.04	66.8	0.0242	0.218	1.61	0.548	0.0269	0.051
2.91	68.3	0.0262	0.101	1.89	86.4	0.0234	0.236	1.30	1.09	0.0248	0.085
2.60	101	0.0266	0.112	1.64	136	0.0234	0.307				
2.29		0.0263	0.184	1.48	187	0.0225	0.374				
				1.36	229	0.0231	0.487				

[a] In the stopped-flow experiment, the solution containing the ligand Hamac and an excess of the metal perchlorate at pH 5−6 was mixed with perchloric acid of variable concentration. [b] $[Co^{2+}] = 1 \times 10^{-2}$ M, [Hamac] = 7.5×10^{-5} M, monitoring at 275 nm. [c] $[Cu^{2+}] = 5 \times 10^{-4}$ M, [Hamac] = 7.5×10^{-5} M, monitoring at 325 nm. [d] $[Ni^{2+}] = 7.5 \times 10^{-3}$ M, [Hamac] = 7.5×10^{-5} M, monitoring at 275 nm. [e] pH after mixing. [f] As obtained by computer-fitting of eq 6 to the exponential absorbance/time data. [g] Initial drop in absorbance; too fast to be followed by the stopped-flow technique.

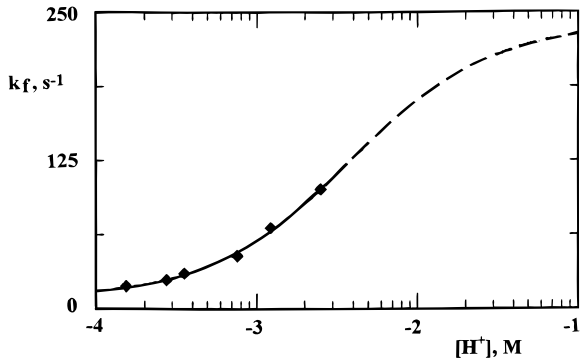

Figure 6. Plot of the experimental rate constant k_f vs log[H^+] according to eq 12 for the fast step of the acid dissociation of the species Co(amac)$^+$ at 298 K.

leads to rate constants k_2 and k_0.[39] According to Scheme 1, the observed pH dependence of k_2 is due to the participation of the enolate in complex formation. Alternatively, the dependence of k_2 on pH could also be due to the mono hydroxo species M(OH)$^+$ being involved. The acidity of the hydrated cations M^{2+}, as described by their pK* values,[40] increases from Ni^{2+} (10.3) to Co^{2+}(9.7) to Cu^{2+}(7.7).[41] At least for copper it is therefore conceivable that complex formation takes place according to (13)−(15). For [M^{2+}] = constant = $[M^{2+}]_0$, [H^+]

$$M^{2+} \overset{K^*}{\rightleftharpoons} M(OH)^+ + H^+ \qquad (13)$$

$$M^{2+} + HE \xrightarrow{k_{HE}} ME^+ + H^+ \qquad (14)$$

$$M(OH)^+ + HE \xrightarrow{k_{OH}} ME^+ + H_2O \qquad (15)$$

= constant ≥ 10^{-5} M, and [M(OH)$^+$] ≪ [M^{2+}], the corresponding rate law is given by (16). Rate constants k_{HE} and k_{OH}, as

$$d[ME^+]/dt = k_2[M^{2+}]_0([HE]_0 - [ME^+]) \qquad (16a)$$

$$k_2 = k_{HE} + k_{OH}K^*/[H^+] \qquad (16b)$$

obtained from the plot of k_2 vs K*/[H^+], are also listed in Table 9 for M = Cu. The ratio k_{OH}/k_{HE} is found to be 2.3×10^4, which is too high to make sense.[42] The interpretation of the pH dependence of k_2 on the basis of reactions (13)−(15) is therefore rejected. The interpretation based on Scheme 1 is obviously more appropriate. Support for this comes also from the comparison of the parameters K_1 and k_E/k_{-E}. Complex formation constant K_1, as determined by spectrophotometric titration (see Experimental Section), should agree with the ratio k_E/k_{-E}, as obtained kinetically from the study of complex formation and dissociation, respectively. The data listed in Table 9 show that K_1 and k_E/k_{-E} differ by factors of about 4 (Ni), 2.4 (Co), and 3.4 (Cu), which are acceptable in view of the different methods applied.

In a general sense, the results of the present study are in line with those of earlier studies on complex formation with β-diketones.[1] It is found that the enolate of Hamac reacts faster with a given metal than the enol, $k_E > k_{HE}$, and that there is a strong metal effect on the rate of complexation with both species, namely $Cu^{2+} \gg Co^{2+} > Ni^{2+}$. The more specific questions to be addressed concern the aspect of rate-control through water exchange on the metal (Eigen−Wilkins mechanism) and the aspect of first bond formation versus second bond formation (chelate ring closure).

Rate constants k_{ex} for water exchange on the metal are listed in Table 9. In the framework of the Eigen−Wilkins mechanism for complex formation with monodentate ligands X it is expected that k_i, the rate constant for the interchange step (X substitutes coordinated H_2O), is close to k_{ex}. In the present study, $k_{i,HE}$ can be estimated according to $k_{HE} = k_{i,HE}K_{os}$ (see Table 9). The ratio $k_{i,HE}/k_{ex}$ ranges from 1.9×10^{-3} (Ni) to 6.8×10^{-5} (Cu). It is much too small to be indicative of solvent exchange controlling the rate of the reaction of HE with the metal. Rate constant k_E however leads to $k_{i,E}/k_{ex} = 0.32$ for copper, which would allow us to invoke solvent exchange to control the reaction of the enolate with copper. Surprisingly, for cobalt

(39) Rate constant k_0, describing the back reaction ($k_0 \equiv k_{-HE}[H^+]/K_{MEH}$), is obtained from the intercept with large limits of error, so that the detailed discussion of its size does not make much sense.

(40) The parameter pK* describes the equilibrium $M^{2+}(aq) \rightleftharpoons M(OH)^+ + H^+$.

(41) Smith, R. M.; Martell, A. E. *Critical Stability Constants*; Plenum Press: New York, 1976; Vol. 4, p 6.

(42) Rate constant k_{ex} for the exchange of coordinated water is a measure for the reactivity of hydrated metal ions M^{q+} toward ligand substitution. The ratio $k(M(OH)^{2+})/k_{ex}(M^{3+})$ is found to be on the order of 500 for M = Cr, Fe, and Ga.[43] To our knowledge there are no data available for water exchange in divalent metal cations and the corresponding monohydroxo species, i.e. for the ratio $k_{ex}(M(OH)^+)/k_{ex}(M^{2+})$.

(43) Van Eldik, R. Ed. *Inorganic High Pressure Chemistry*; Studies in Inorganic Chemistry 7; Elsevier: Amsterdam, 1986; pp 82 and 85.

(44) Ducommun, Y.; Zbinden, D.; Merbach, A. E. *Helv. Chim. Acta* **1982**, *65*, 1385.

(45) Powell, D. H.; Helm, L.; Merbach, A. E. *J. Chem. Phys.* **1991**, *95*, 9258.

(46) The calculated ion pair formation constants K_{OS} for divalent 3d cations pairing with singly charged anions are 0.81 M^{-1} for I = 0.1 M and 0.54 M^{-1} for I = 1.0 M for the medium water and 298 K.[47]

(47) Jordan, R. B. *Reaction Mechanisms of Inorganic and Organometallic Systems*; Oxford University Press: Oxford, England, 1991; p 33.

and nickel the ratio $k_{i,E}/k_{ex}$ is smaller by about one order of magnitude (0.039 and 0.048, respectively). Considering the pK* values of the aqua metal ions under study, one is tempted to suggest that the reaction of the enolate with the M^{2+} cation is "acidity-assisted" in the sense that formation of the first M−O bond with the enolate is initiated and facilitated by the formation of a more or less strong hydrogen bond between a coordinated water molecule and the attacking enolate. This would at least explain as to why the ratio $k_{i,E}/k_{ex}$ is highest for copper (pK* = 7.7) and lower for cobalt (pK* = 9.7) and nickel (pK* = 10.3).[48] In summary, the ratio $k_{i,E}/k_{ex} = 0.32$ for copper could suggest the operation of the Eigen−Wilkins mechanism with formation of the first Cu−O bond with the enolate E^- being controlled by the rate of water exchange on the copper. The low values of $k_{i,E}/k_{ex}$ obtained for cobalt and nickel however are not in line with this interpretation and point to intermolecular hydrogen bond formation as being rate-affecting.

For the reaction of the enol HE with the metal it is found that $k_{i,HE}/k_{ex} \ll 1$, which means that the rate of this reaction is obviously not governed by the rate of solvent exchange on the metal cation. In addition, the ratio $k_{i,HE}/k_{ex}$ is more strongly metal-dependent than the ratio $k_{i,E}/k_{ex}$ (see Table 9). The existence of the k_{HE} pathway as such indicates, however, that the rate-determining step occurs prior to the formation of the second M−O bond with the entering ligand. The question of why the formation of the first M−O bond with the enol HE occurs so slowly is as open to speculation as it has been all the time.[1] It is reasonable to assume that the enol HE is substantially stabilized by intramolecular hydrogen bond formation, producing a six-membered heterocyclic ring. The symmetry of this ring and the charge distribution within it will be rather close to the symmetry and charge delocalization in the mono complex species ME^+. This means that the reaction of the enol HE with the metal corresponds to the substitution of the cation H^+ by the cation M^{2+}. From the kinetic point of view, this process is found to be a second-order reaction. Its slowness cannot simply be due to the fact that the enol is a poor entering ligand.[49] If that were the case, the ratio k_{HE}/k_{ex} should not be so much metal-dependent as it is. Some characteristic property of the metal has to be involved, and one might again suggest that the different acidity of the hydrated metal cations is essential. The most acidic copper ion is the one providing most easily the mono hydroxo species, which is able to support the breaking of the hydrogen bond stabilized cyclic enol.

The acid hydrolysis of the species $M(amac)^+ = ME^+$ is triphasic. Very fast proton addition, leading to the cation MEH^{2+}, is followed by the dissociation of MEH^{2+} and ME^+ to form M^{2+} and the enol HE, which finally ketonizes. The pH dependence of the dissociation reaction leads to the acid dissociation constant K_{MEH} (see Scheme 1) for copper (K_{MEH} = 0.22 M) and cobalt (K_{MEH} = 0.0038 M). In the case of nickel one can estimate $K_{MEH} \geq 0.5$ M. These data mean that the species $Co(amac)^+$ is the most basic one and that the species $Ni(amac)^+$ and $Cu(amac)^+$ are much weaker proton acceptors. From the chemical point of view one has to assume that the cation MEH^{2+} corresponds to a species in which the enol Hamac coordinates in a monodentate fashion. This unstable species is involved in complex formation as well as in complex dissociation as an intermediate.

Conclusions

The β-diketone Hamac, a modified acetylacetone with a *N*-acetylamido group in the 3-position, is very soluble in water, strongly enolized ([enol]/[ketone] = 2.4), and rather acidic (pK_a = 7.1). Hamac coordinates metal ions such as Cu^{2+} in a normal fashion, i.e. via the two diketo oxygens. It follows from the kinetic investigation of the formation of the mono complex $M(amac)^+$ with M = Ni, Co, and Cu at variable pH that the enol tautomer of Hamac, HE, and the enolate anion, E^-, are the reactive species to form $M(amac)^+$, with second-order rate constants $k_E > k_{HE}$. In both, k_{HE} and k_E are strongly metal-dependent, the order of reactivity being Ni < Co ≪ Cu. The kinetic data suggest that (i) in the reaction of the divalent metal ions M^{2+} with both the enol HE and the enolate E^- formation of the first M−O bond is rate-controlling and (ii) the acidity of the coordinated water in the cations M_{aq}^{2+} is rate-affecting. The study of the acid dissociation leads to the equilibrium constant K_{MEH} for the protonation of the complex ME^+. The protonated species MEH^{2+} with Hamac coordinated in a monodentate fashion is an intermediate in both complex formation and complex dissociation.

Acknowledgment. Sponsorship of this work by the Deutsche Forschungsgemeinschaft, Verband der Chemischen Industrie, e.V., and Otto-Röhm-Stiftung is gratefully acknowledged. The authors appreciate the expertise of Dr. Klaus Jürgen Wannowius in computer handling of the kinetic data.

Supporting Information Available: Tables S1−S4, listing complete crystallographic data, calculated coordinates of hydrogens, distances and angles, and thermal parameters (5 pages). Ordering information is given on any current masthead page.

IC950272G

(48) Interestingly, the ratio k_E/k_{HE} also follows qualitatively the acidity of the aqua cations in that k_E/k_{HE} for copper is by a factor of 183 and 23 larger than for nickel and cobalt, respectively.

(49) It is of interest to note that rate constants k_{HE} for the reaction of Ni^{2+} ions with the enol tautomers of Hacac, Hamac, Hhptd,[20] Htfpd,[20] and Htftbd[20] lie within the narrow range of 1.7 (Htfpd) to 19.3 (Hacac) M^{-1} s^{-1} (298 K).[50]

(50) The data for k_{HE} were taken from Table 2 of ref 1.